Dynamics of Atmospheres and Oceans xxx (2009) xxx–xxx

Contents lists available at ScienceDirect

Dynamics of Atmospheres and Oceans

journal homepage: www.elsevier.com/locate/dynatmoce

The effects of mixing and spreading on density in near-field river plumes

Robert D. Hetland

Dept. of Oceanography, Texas A&M University, 3146 TAMU, College Station, TX 77843-3146, United States

ARTICLE INFO

Article history:
Received 12 June 2008
Received in revised form 20 November 2008
Accepted 21 November 2008
Available online xxx

Keywords:
River plumes
Plume dilution
Plume spreading

ABSTRACT

Water mass modification in surface-trapped, near-field river plumes is examined using a 1.5-layer reduced gravity model and a three-dimensional numerical model. Solutions to the layer model are shown to be qualitatively similar to previous observations and three-dimensional simulations of near-field plumes. Analytic analysis of the layer model demonstrates how the near-field plume is controlled by the competing processes of mixing and spreading. The two models are then used to explore the parameter space dependence of density changes within the near-field plume and their associated cross-shore length scales. Both the magnitude of density changes and their length scales are proportional to either estuarine discharge or fresh water discharge; density changes are also inversely proportional to the estuary mouth width. One surprising feature of the parameter space solutions is that the density of water exiting the near-field plume, a measure of the net dilution of the entire near-field plume, is shown to be inversely proportional to local mixing rates. This is because when local mixing is lower, the influence of plume spreading becomes greater; this spreading accelerates the plume, requiring more net mixing to bring the plume back to subcritical flow.

1. Introduction

Theories that describe shelf-scale buoyant plume structure rely on relating the properties at the source, for example the density anomaly and discharge magnitude, to these same properties further downstream (e.g., Yankovsky and Chapman, 1997; Fong and Geyer, 2002). However, the density of the

E-mail address: hetland@tamu.edu.

0377-0265/$ – see front matter © 2008 Elsevier B.V. All rights reserved.
doi:10.1016/j.dynatmoce.2008.11.003

outflow depends on the mixing history of a water parcel as it travels through the estuary and coastal waters; purely fresh river discharge is strongly modified by entrainment of oceanic water in the estuary and near-field river plume (Hetland, 2005). Just as the estuary acts as a source for the near-field plume, the near-field plume acts as a source for the far-field. Mixing in the near-field plume region, typically much more energetic than mixing in the far-field plume beyond, can alter shelf-scale buoyant plume structure by changing the effective source properties.

The near-field is defined in this paper as the area over which the estuarine outflow is supercritical, where advection and shear mixing dominate the dynamics. Also, here, the shape of the buoyancy source is important in determining the shape of the near-field plume flow structure. This is distinct from the far-field river plume where the earth's rotation, wind, and background flow dominate the evolution of the plume, where the rotational deformation radius and shelf bathymetry determine the cross-shore spatial scales of the plume (e.g., Yankovsky and Chapman, 1997; Lentz and Helfrich, 2002).

The characteristics of estuarine outflow as a function of fresh water inputs and mixing within the estuary have been studied extensively (e.g., Stommel and Farmer, 1953; Hansen and Rattray, 1965; Chatwin, 1976; MacCready et al., 2002; Hetland and Geyer, 2004; MacCready, 2007). These studies demonstrate how fresh river water is transformed within the estuary through mixing as a function of the tidal forcing and geometry of the estuary. For example, the steady model of estuarine circulation developed by Hansen and Rattray (1965) shows how estuarine salinity structure is controlled by river discharge and mean tidal mixing.

There has been much previous work examining similar functional relationships on engineering-scale jets and plumes, for example, positively buoyant plumes directed upward from a circular source reviewed in textbooks such as Turner (1973) and Fischer et al. (1979). (The near- and far-field are referred to as the jet and plume, respectively, for engineering-scale flows.) Engineering-scale jets and plumes are defined here to have a cross-section aspect ratio of $\mathcal{O}(1)$, and are small enough that the earth's rotation is dynamically unimportant. Fischer et al. (1979) show how fundamental jet and plume properties, such as length scales and dilution rates, depend on properties of the source outflow, such as the mass, momentum, and buoyancy fluxes. These properties provide a useful framework for analyzing geophysical scale plumes.

However, results for engineering-scale jets and plumes should not be directly applied to geophysical-scale plumes, as there are many fundamental differences between the two. Geophysical plumes have a very small $\mathcal{O}(10^{-3} - 10^{-4})$ cross-sectional aspect ratio. The small aspect ratio means that entrainment of ambient water is primarily a vertical process, lateral entrainment is relatively small. The Froude number is always $\mathcal{O}(1)$ in geophysical plumes, whereas it can be much larger than one at the source of an engineering-scale jet. Entrainment increases as an engineering-scale plume transitions from jet to plume (as a function of distance from the source); geophysical far-field plumes tend to form coastally trapped boundary currents where entrainment is quite small (Garvine, 1999; Hetland, 2005).

This paper examines the net change in density through the near-field plume, or the net plume dilution through the near-field region, as a function of the estuary mouth width and discharge magnitude. Although similar studies exist for engineering-scale jets and plumes, for example the outflow from a submerged pipe, no such study has been done for geophysical-scale plumes. The results show that the near-field plume behaves in some ways similar to an engineering-scale jet, where the length scale of the near-field is a function of the momentum flux and buoyancy flux. However, unlike an engineering-scale jet, the aspect ratio of the source water is also important in determining the plume length scales and net dilution through the near-field plume.

To investigate density changes in the near-field plume, two models are used. First a simple layer model is developed that can be used to scale changes in the near-field plume density structure to different discharges and source widths. The layer model offers some insight into the physical reasons behind the plume response. A three-dimensional primitive equation model is then used to evaluate the scaling predicted by the layer model.

2. Background

Immediately after fresh water leaves the estuary, it begins to spread, as it is no longer confined to the estuary channel. This spreading causes the plume to shoal, by continuity. (Note, if the estuarine

Please cite this article in press as: Hetland, R.D., The effects of mixing and spreading on density in near-field river plumes. Dyn. Atmos. Oceans (2009), doi:10.1016/j.dynatmoce.2008.11.003

outflow is still in contact with the bottom at the estuary mouth, the point at which it loses contact with the bottom can be considered as the beginning of the plume, see MacDonald and Geyer, 2005.) The shoaling pycnocline is associated with a drop in the sea surface height, assuming relatively still water beneath the buoyant plume, and by the Bernoulli principle the drop in surface pressure is associated with an acceleration of the plume. Observations by Wright and Coleman (1971), MacDonald and Geyer (2004), and MacDonald et al. (2007) show that buoyant water leaving a narrow estuary rapidly shoals over a distance of a few channel widths

The accelerating plume increases the shear at the base of the plume, eventually triggering shear instabilities, and entrainment of low-momentum, high-density ambient water into the buoyant plume. Entrainment is strongest near the point where the plume is thinnest. Mixing in this region can be quite energetic; MacDonald et al. (2007) estimate maximum dissipation rates just under 10^{-3} m^2 s^{-3}. After the point of maximum entrainment, entrainment continues decelerates the plume, which then gradually returns to subcritical as it thickens, over a distance of a few tens of channel widths.

Thus, spreading is the dominant mechanism up to the point where the plume is the thinnest, and entrainment is dominant beyond. However, both spreading and entrainment act throughout the near-field plume, and these two processes may influence each other. For example, spreading can act to enhance mixing by thinning, and thereby accelerating, the plume. This acceleration provides more kinetic energy for the formation of shear instabilities. Entrainment lowers the density anomaly of the plume, which, as discussed below, will alter the spreading rate.

Based on their observations, Wright and Coleman (1971) relate the horizontal spreading of the plume to the internal gravity wave speed, noting that the front expands at approximately the internal gravity wave speed, $\sqrt{g'h}$, where $g' = g\Delta\rho/\rho_0$ is the reduced gravity, $\Delta\rho$ is the local density difference between plume and ambient water, and h is the thickness of the buoyant layer. This result was confirmed by Hetland and MacDonald (2008), who show that the spreading rate of the Merrimack River near-field plume is consistent with the local internal gravity wave speed. That is, following a water parcel from the source, initially the same width as the estuary mouth, the edges of the water parcel propagate perpendicular to the flow direction at approximately the local reduced gravity phase speed. Of course, the lateral boundaries of a real plume are not so well defined. However, Hetland and MacDonald (2008) show that the spreading rate in the core of the near-field plume is still determined by the interior density anomaly as if it were a uniform slab, spreading as in a dam break problem.

Reduced gravity layer models have often been used to describe river plume flow in general (e.g., Fong and Geyer, 2001; Yankovsky and Chapman, 1997; McCreary et al., 1997; Hetland, 2005), and near-field plume structure in particular (notably, Garvine, 1982, 1984, 1987; O'Donnell, 1990). Many layer models of the near-field plume have focused on an expanding tidal pulse of low salinity water leaving the estuary, similar to the observations of Luketina and Imberger (1987). These models all focus on frontal position and mixing at the frontal boundary; for example, Garvine (1982, 1984, 1987), assumed inviscid dynamics in the interior of the plume, with the only mixing at the frontal boundary condition.

O'Donnell (1990) investigated plume expansion using numerical solutions of a two-dimensional layer model that included entrainment within the interior of the plume in addition to an entraining frontal boundary condition. O'Donnell's model is similar to the layer model developed below in that it includes both plume spreading and entrainment inside the plume. However, O'Donnell's model is much fuller; it is time dependent and includes the effects of rotation and background flow on the plume. Thus, O'Donnell's model offers a much more realistic simulation of the evolution of an individual plume. However, O'Donnell's numerical setup and analysis of the problem is different than that presented here in two respects: First, the source (what would here be defined as the estuary mouth) was semicircular, so that the plume never separated from the coastline. Second, O'Donnell focused primarily on the time-dependent formation of the plume and plume front. However, the results are similar to those presented here in that the plume structure behind the propagating front is relatively stable (see, e.g., O'Donnell's Fig. 7). An advantage of the approach used in this paper is that the system of equations is simple enough such that it is possible to derive scaling laws; O'Donnell's approach is physically more realistic, but less tractable analytically.

Davis (1999) describes a model (PDSG) that is intended to simulate real buoyant discharges at large engineering scales, or small geophysical scales. The PDSG model is similar to the layer model presented below in that the structure of the plume is assumed to vary primarily along the main axis of the plume,

Please cite this article in press as: Hetland, R.D., The effects of mixing and spreading on density in near-field river plumes. Dyn. Atmos. Oceans (2009), doi:10.1016/j.dynatmoce.2008.11.003

but the lateral and vertical structure of the plume are more realistic; the PDSG model uses specified structure functions to extrapolate the core of the plume horizontally and in depth. Changes in plume width are caused by gravitational expansion as well as through horizontal and vertical entrainment. Although rotation is not included, the PDSG model includes many important processes that affect real discharge plumes, such as heat loss to the atmosphere, and the presence of background flow. However, due to its complexity, and the fact that many of the processes are specified using empirically determined constants, it is difficult to derive even partial analytical solutions from the PDSG model.

In contrast, the layer model presented below is intended to examine plume scales over a wide variety of forcing conditions; the simplicity of the model also allows some analytical scales of the plume to be derived. The layer model contains the simplest possible representation of the basic elements of the near-field plume: entrainment and plume spreading. The layer model is intended to be similar in spirit to the models of estuarine circulation by Hansen and Rattray (1965) and Chatwin (1976); that is, instructive for examining the basic dynamics of the system, but not intended for realistic simulations. Previous studies (MacDonald and Geyer, 2004; MacDonald et al., 2007; Hetland and MacDonald, 2008) have shown that rotation is not a primary factor in near-field plume development, so rotation is not included.

Observations (Wright and Coleman, 1971; MacDonald and Geyer, 2004; MacDonald et al., 2007) and numerical simulations (O'Donnell, 1990; Hetland, 2005; Hetland and MacDonald, 2008) of near-field plumes show there is considerable entrainment within the core of the plume, away from frontal boundaries. Also, the timescales of flow in this region can be as low as a few hours, so that it is possible for the near-field plume to come to a steady state on tidal timescales. Both O'Donnell (1990) and Hetland and MacDonald (2008) show that the near-field plume comes to a steady state almost immediately following the plume front. Thus, when examining the core of the near-field plume, the steady-state assumption is justified, and simplifies the mathematics considerably.

3. Theory

A simple layer model is developed that includes plume spreading and entrainment. The plume is assumed to be in a steady state and to have separated from the coast at the estuary mouth. Plume spreading beyond the mouth results in a pie-shaped near-field plume region, as shown in the layer model setup (Fig. 1). Hetland and MacDonald (2008) show that properties within the near-field, within a few kilometers of the estuary mouth, plume are a function of radial distance from the mouth (although for convenience, distance along the plume centerline is used here as the independent variable). Thus, plume width can be defined as the distance between two streamlines bracketing the core of the near-field plume, and the properties within these streamlines may be approximated as constant.

A buoyant fluid is introduced into a reservoir through a rectangular gap in a coastal wall with a width W_0, representing an estuary mouth. The estuarine outflow is steady, with a velocity u_0 and density anomaly $\Delta\rho_0$ at the point where the flow enters the coastal ocean. The quiescent ambient water in the coastal ocean has a uniform density, ρ_0. The axes are oriented such that the origin is

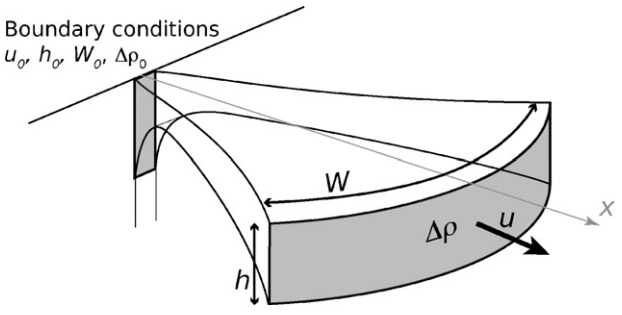

Fig. 1. The setup of the layer model showing model variables and coordinate system.

Please cite this article in press as: Hetland, R.D., The effects of mixing and spreading on density in near-field river plumes. Dyn. Atmos. Oceans (2009), doi:10.1016/j.dynatmoce.2008.11.003

located at the center of the gap, with positive x directed seaward from the source. After the flow enters the ocean, it separates from the coast, spreads, thins, and entrains background water.

The notion of hydraulic control at the estuary mouth dates back to Stommel and Farmer's (1953) overmixing theory, later formalized and extended by Armi and Farmer (1986). Based on these theoretical studies and observations, the mouth is assumed to act as a constriction, and the flow is assumed to be exactly critical at the estuary mouth where the flow enters the ocean. Thus, the vertical thickness of the outflow at the estuary mouth, h_0, is specified such that the Froude number at $x = 0$ is one,

$$Fr|_{x=0} \equiv \frac{u_0}{\sqrt{g'_0 h_0}} = 1, \tag{1}$$

where $g'_0 \equiv g\Delta\rho_0/\rho_0$ is the reduced gravity of the flow at the estuary mouth. (Values at the boundary condition location $x = 0$ are noted by a subscript 0 throughout.) This condition may be extended to include source water with a Froude number greater than one. All of the results remain valid, but the functional dependencies described then also need to include the parameter $Fr_0 = Fr(x = 0)$.

Continuity and density conservation may be used to relate the local flux of water at some point away from the coast to these constant estuary outflow properties,

$$Q\Delta\rho = h\,u\,W\,\Delta\rho = h_0\,u_0\,W_0\,\Delta\rho_0 = Q_0\Delta\rho_0, \tag{2}$$

where h is the active upper-layer thickness, u the upper-layer radial velocity away from the estuary mouth, $\Delta\rho$ the density anomaly of the upper layer, and Q_0 is the volume flux leaving the estuary. This statement asserts that the fresh water flux is constant for all x. When entrainment is included, the local mass flux of the plume, Q, will increase away from the source.

Assuming a steady state enables replacing the total derivative with a local advection term,

$$\frac{\mathrm{D}}{\mathrm{D}t} = u\frac{\partial}{\partial x}, \tag{3}$$

so that conservation of density and momentum in a non-rotating buoyant layer are

$$u\frac{\partial\rho}{\partial x} = \frac{w_e\,\Delta\rho}{h}, \tag{4}$$

$$u\frac{\partial u}{\partial x} = -g'\frac{\partial h}{\partial x} - h\frac{\partial g'}{\partial x} - \frac{w_e\,u}{h}, \tag{5}$$

where $g' \equiv g\Delta\rho/\rho_0$ is the (variable) reduced gravity, and w_e is an entrainment velocity. Note that it is important to include the contribution of the variable density field to the pressure gradient, as the density of the outflow will change in the x-direction.

An entrainment velocity, w_e, is defined to represent mixing of density and momentum from the lower layer into the upper layer. There are a number of ways to define the entrainment velocity, often based on the internal, densimetric Froude number (e.g., Ellison and Turner, 1959; Turner, 1973; Cenedese et al., 2004). Although many different entrainment parameterizations were investigated, the results presented here use a constant entrainment rate, $\delta = w_e/u$. This approximation is often used in engineering-scale plumes, simplifies the mathematics, is consistent with $Fr = \mathcal{O}(1)$, and produces a plume density structure similar to the three-dimensional model.

In classic models of hydraulic flow, width is specified so that the problem has a single independent variable, oriented along-channel (see Armi and Farmer, 1986; Turner, 1973; Baines, 1995). Here, the width of the near-field plume is a variable that must be solved. Previous studies (Wright and Coleman, 1971; Hetland and MacDonald, 2008) have shown that the separated plume spreads perpendicular to the flow direction with a rate proportional to the local internal gravity wave speed, $c = \sqrt{g'h}$. Thus, following a parcel of water, the local rate of change in plume width, W, is

$$\frac{\mathrm{D}W}{\mathrm{D}t} = u\frac{\partial W}{\partial x} = 2\sqrt{g'h}. \tag{6}$$

The factor of two is required because the plume is spreading along both edges. Thus, plume spreading is parametrized by assuming that the front expands in the along-shore direction at the local internal

Please cite this article in press as: Hetland, R.D., The effects of mixing and spreading on density in near-field river plumes. Dyn. Atmos. Oceans (2009), doi:10.1016/j.dynatmoce.2008.11.003

gravity wave speed. This allows the system of equations to be written using a single independent variable, oriented cross-shore. Note, there is no need to consider entrainment across the lateral boundaries (as in, e.g., O'Donnell, 1990) since the flow and flow characteristics are parallel to the plume edges.

The above equations may be written as a system of linear, first-order differential equations:

$$\frac{\partial \Delta\rho}{\partial x} = -\Delta\rho \frac{w_e}{u\,h} \tag{7}$$

$$\frac{\partial W}{\partial x} = 2Fr^{-1} \tag{8}$$

$$\frac{\partial u}{\partial x} = \frac{u}{(1 - Fr^{-2})}\left[\frac{1}{\Delta\rho}\frac{\partial \Delta\rho}{\partial x} + Fr^{-2}\frac{1}{W}\frac{\partial W}{\partial x}\right] \tag{9}$$

$$\frac{\partial h}{\partial x} = -h\left[\frac{1}{\Delta\rho}\frac{\partial \Delta\rho}{\partial x} + \frac{1}{W}\frac{\partial W}{\partial x} + \frac{1}{u}\frac{\partial u}{\partial x}\right] \tag{10}$$

where the internal Froude number, $Fr = u/\sqrt{g'h}$, has been used where appropriate. The characteristics of the solutions need to be monodirectional so, technically, solutions are valid only where the flow is supercritical, $Fr \geq 1$. Eq. (10) comes from an x derivative of Eq. (2). Eq. (9) comes from substituting Eq. (10) into Eq. (5) and rearranging terms; this is necessary in order to cast the right-hand-side such that it only depends on x derivatives of W and $\Delta\rho$. Then, the right hand sides of all of the equations can be determined given only the state vector ($\Delta\rho$, W, u, h).

Eqs. (7) through (10) are written in terms of the independent variable x, although real plume properties are a function of radial distance from the estuary mouth (Hetland and MacDonald, 2008). However, since there are no derivatives in the cross-shore (or transverse) direction, the equations are identical whether they are cast in terms of x or radial distance, r. The primary difference is the location of the initial boundary condition, which for a radial coordinate system must be specified at $r = \sqrt{W^2/2}$ for an initial Froude number of one (i.e., the lateral plume fronts both spread at 45° relative to the plume axis).

Eqs. (7) through (10) may be non-dimensionalized using the scales $x = W_0 x^*$, $u = u_0 u^*$, $h = h_0 h^*$, $W = W_0 W^*$, $\Delta\rho = \Delta\rho_0 \Delta\rho^*$, and $Fr = Fr^*$ (i.e., assuming $Fr_0 = 1$), where the subscript 0 represents the initial value of each variable at $x^* = x = 0$, the estuary mouth:

$$\frac{\partial \Delta\rho^*}{\partial x^*} = -\frac{\Delta\rho^*}{h^*}\frac{\delta}{\alpha_0} \tag{11}$$

$$\frac{\partial W^*}{\partial x^*} = 2Fr^{*-1} \tag{12}$$

$$\frac{\partial u^*}{\partial x^*} = \frac{u^*}{(1 - Fr^{*-2})}\left[\frac{\Delta\rho^*_{x^*}}{\Delta\rho^*} + Fr^{*-2}\frac{W^*_{x^*}}{W^*}\right] \tag{13}$$

$$\frac{\partial h^*}{\partial x^*} = -h^*\left[\frac{\Delta\rho^*_{x^*}}{\Delta\rho^*} + \frac{W^*_{x^*}}{W^*} + \frac{u^*_{x^*}}{u^*}\right] \tag{14}$$

The solution depends only on two parameteres: $\delta = w_e/u$, the entrainment rate and $\alpha_0 = h_0/W_0$, the initial aspect ratio of the plume. There is also an implicit dependence on Fr_0; to explicitly include the dependence on Fr_0, replace Fr^* with $Fr_0 Fr^*$. It is important to note, however, that because of the non-linear nature of the system of equations and because of the choice of scales, the non-dimensional variables are not guaranteed to be $\mathcal{O}(1)$. Width, for instance may increase by an order of magnitude or more relative to the initial plume width.

From Eqs. (7) through (10), the gradients of the Froude number with respect to x may be calculated,

$$\frac{\partial Fr}{\partial x} = \frac{uh(Fr^2 + 2) - (3/2)w_e W Fr^3}{Q(Fr^2 - 1)}, \tag{15}$$

Please cite this article in press as: Hetland, R.D., The effects of mixing and spreading on density in near-field river plumes. Dyn. Atmos. Oceans (2009), doi:10.1016/j.dynatmoce.2008.11.003

non-dimensionally as,

$$\frac{\partial Fr^*}{\partial x^*} = \frac{\alpha^*(Fr^{*2}+2) - (3/2)(\delta/\alpha_0)Fr^{*3}}{h^*(Fr^{*2}-1)}, \tag{16}$$

where $\alpha^* = h^*/W^*$ is the non-dimensional aspect ratio of the plume as a function of x^*. Again, the only parameter that determines the structure of the Froude number is δ/α_0.

In the case with critical or supercritical initial flow, $Fr_0 \geq 1$, and no entrainment, $w_e = \delta = 0$, the Froude number always increases due to plume spreading; entrainment must be included for the Froude number to decrease. Thus, this equation quantifies the competition between spreading, which tends to increase the Froude number, and entrainment, which tends to decrease the Froude number. The maximum Froude number, where the slope of the Froude number changes sign, is the point where entrainment (the $w_e W$ term in the numerator of (15)) just begins to overwhelm inertia (the uh term).

For solutions to exist, the Froude number must be increasing at $x = 0$, otherwise there is no region of supercritical flow. By Eq. (15), this requires that

$$\frac{2Q_0}{W_0^2 w_e} = 2\alpha_0\delta^{-1} > 1. \tag{17}$$

As expected, wide estuaries or estuaries with weak discharge will not have a supercritical region where this theory will be valid. In other words, only estuaries that are narrow enough, with high enough discharge, will have a near-field plume as defined in this paper.

Likewise, Eq. (9) requires that, when $Fr = 1$ again (i.e., entrainment has reduced the Froude number and returned the flow to subcritical) and after appropriate substitutions to remove derivative quantities,

$$\frac{\Delta\rho_L}{\Delta\rho_0} = 2\left(\frac{Q_L}{w_e W_L^2}\right), \tag{18}$$

where subscript L represents the plume properties at $x = L$, where the plume returns to subcritical conditions. The normalized density anomaly, $\Delta\rho_L/\Delta\rho_0$, is one way to define the net mixing, or plume dilution, that has occurred through the near-field plume. Once the normalized density anomaly is calculated, the transport (Eq. (2)), width (Eq. (18)), thickness, and velocity (using $Fr(x = L) = 1$) can also all be found.

4. Results

4.1. Numerical methods

The layer model is solved with a standard linear systems solver. Table 1 shows the range of parameters used in the solution space. Solutions are integrated out to 50 km, and only the supercritical ($Fr > 1.0$) portion of the solution is considered.

Table 1
The range of parameters used as in the layer model solution. The solution space includes cases that are well outside of the realistic range, but thereby also spans most reasonable values for realistic cases.

	Minimum	Maximum
Specified parameters		
Q_f [$m^3\,s^{-1}$]	10.0	5000.0
$\Delta\rho_0$ [$kg\,m^{-3}$]	1.0	24.0
W_0 [m]	50.0	1000.0
δ	0.001	0.005
Derived parameters		
Q_0 [$m^3\,s^{-1}$]	10.4	125,000.0
h_0 [m]	0.016	590.1
α_0	1.7×10^{-5}	10.3

Please cite this article in press as: Hetland, R.D., The effects of mixing and spreading on density in near-field river plumes. Dyn. Atmos. Oceans (2009), doi:10.1016/j.dynatmoce.2008.11.003

A series of three-dimensional model solutions were also performed using the Regional Ocean Modeling System (ROMS, Shchepetkin and McWilliams, 2005). The domain size is $92 \times 92 \times 10$; the domain size was halved by placing a no-slip wall along what would be the plume centerline. Water was introduced into the domain through a channel eight grid points wide; the width of the channel was varied by varying the grid size, Δx and Δy. Grid resolution was focused near the mouth with five times the resolution of the region far from the mouth. Other numerical details are similar to the realistic simulation of the Merrimack River Plume described by Hetland and MacDonald (2008). Briefly, the MPDATA advection scheme was used with a $k - \epsilon$ turbulence closure and Canuto-A stability functions (similar turbulence closure configurations were also used by Canuto et al., 2001; Burchard and Bolding, 2001; Warner et al., 2005). The initial conditions were quiescent with a weak temperature stratification. Standard Orlanski-style radiation conditions were used to allow the plume to leave the domain. The model was forced with a fresh water flux at the landward end of the estuary between $Q_f = 10$ and $2000\,\mathrm{m^3\,s^{-1}}$, with an estuary width between $W = 50$ and 3000 m. Some mixing occurs within the estuary, so that at the estuary mouth, the outflow is between $Q_0 = 12$ and $7356\,\mathrm{m^3\,s^{-1}}$. Although the model was capable of resolving instabilities with a lateral scale on the order of the estuary mouth, no such instabilities were observed. This is because of the very low aspect ratio of the plume. It is possible that with higher resolution, smaller scale instabilities would develop, but it is not likely that these would strongly influence the larger scale structure of the plume as a whole.

It was important to run the simulations with enough horizontal and vertical resolution. Without adequate resolution, numerical diffusion degraded the solutions. It should be noted that numerical diffusion and dispersion can be caused by grid-scale instabilities, as discussed by Hetland (2005), but also from (stable) numerical advection between cells, as discussed by Burchard and Rennau (2008).

4.2. Comparison of the layer model to three-dimensional models

The layer model and the three-dimensional model are compared for an idealized and realistic model configuration. Fig. 2 shows a the comparison of the layer model with an idealized three-dimensional model configuration, for the case with $2000\,\mathrm{m^3\,s^{-1}}$ fresh water flow into the domain and a 500 m wide estuary mouth. The upper layer density, $\Delta\rho$, is calculated within the three-dimensional model by calculating a ratio of the first moment of the density anomaly squared divided by the seconds moment,

$$\Delta\rho\, h = \int_{-\infty}^{\eta} (\rho_0 - \rho)\,\mathrm{d}z \tag{19}$$

$$\Delta\rho\, h^2 = \int_{-\infty}^{\eta} (\rho_0 - \rho)\, z\,\mathrm{d}z \tag{20}$$

where z is the depth, η is the free surface, h is the upper layer thickness, ρ is the three-dimensional density field calculated by the model, and ρ_0 is the background density. This method was used by Arneborg et al. (2007) and Umlauf et al. (2007) to examine dense gravity currents in the Baltic Sea.

The layer model solution differs from the three-dimensional solution in some important aspects. Some of these differences, particularly differences in the lateral structure, are due to the fact that these are simply two very different models, and an exact comparison is not possible. However, the some of the differences in the density anomaly are most likely because the entrainment parameterization in the layer model does not take into account changes in the Richardson number. Despite this, the layer model does capture the bulk scales of the three-dimensional model. The width of the plume calculated by the layer model is associated with a break in the upper layer density contours. Also, the final far-field upper layer density predicted by the layer model is within 40% of the three-dimensional model upper layer density, even though the density changes by a factor of about five.

4.3. Average entrainment rates in the three-dimensional model

In order to place the three-dimensional numerical model results within the context of the layer model theory, turbulent diffusion rates in the three-dimensional model must be related to entrainment

Please cite this article in press as: Hetland, R.D., The effects of mixing and spreading on density in near-field river plumes. Dyn. Atmos. Oceans (2009), doi:10.1016/j.dynatmoce.2008.11.003

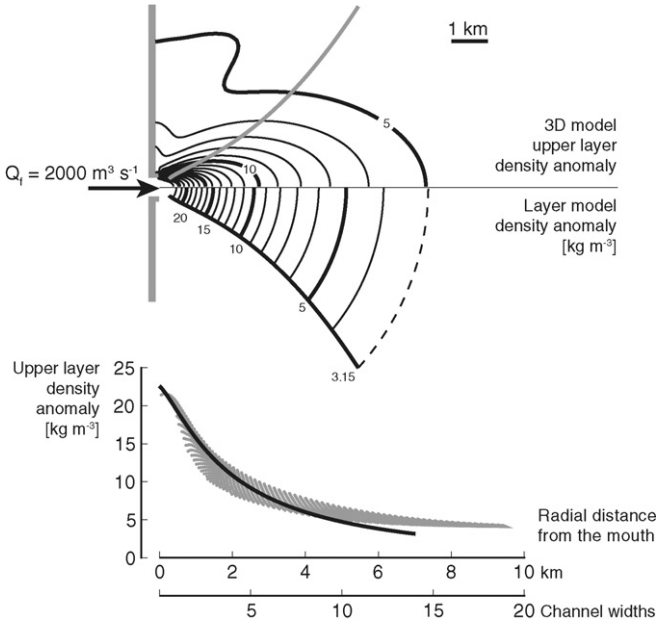

Fig. 2. The upper panel shows a split view of the the layer thickness estimated from the three-dimensional model above and the layer mode thickness below. The gray line shows the plume width estimated from the layer model, mirroring the lateral plume boundary below. The lower panel compares the upper layer density anomaly of the plume (larger is fresher) as a function of radial distance from the mouth.

velocities in the layer model. A method for relating three-dimensional diffusion to a layer model entrainment velocity using was developed by Hetland (2005), who used this method to investigate time-dependent entrainment in a wind-driven buoyant plume. Here the situation is much simpler. For a given isopycnal within a steady plume, mass balance requires that

$$Q_f = \langle w_e \rangle A \tag{21}$$

where Q_f is the volume flux of the fresh water river discharge, $\langle w_e \rangle$ is the average entrainment velocity across the isopycnal, and A is the surface area of the isopycnal. Eq. (21) will give the *average* entrainment across the entire isopycnal surface. However, the entrainment rate may change considerably through the plume. Hetland (2005) suggests that different dynamical regions within the plume can be identified by the upper layer salinity. For the case of the near-field plume, entrainment is expected to be highest near the source, where the upper layer salinity is lowest; entrainment will then decrease as the upper layer salinity increases (MacDonald et al., 2007). This assumption is similar to the assumption in the layer model that dynamical properties are uniform across the plume arc. Hetland (2005) also develops a method to calculate local entrainment velocity as a function of upper layer salinity, s; for a steady state plume

$$Q_f = s\, w_e \frac{\partial A}{\partial s}. \tag{22}$$

where Q_f is the fresh water river flux and $A(s)$ is the area enclosed by a particular isohaline contour of the upper layer salinity. This equation may be heuristically derived by taking the difference of Eq. (21) multiplied by two salinities representing two neighboring isohaline surfaces. The entrainment velocity calculated represents the average entrainment over the region where the two surfaces do not overlap. The upper layer salinity and upper layer density anomaly are related by

$$\frac{s}{s_0} = 1 - \frac{\Delta\rho}{\Delta\rho_f} \tag{23}$$

Please cite this article in press as: Hetland, R.D., The effects of mixing and spreading on density in near-field river plumes. Dyn. Atmos. Oceans (2009), doi:10.1016/j.dynatmoce.2008.11.003

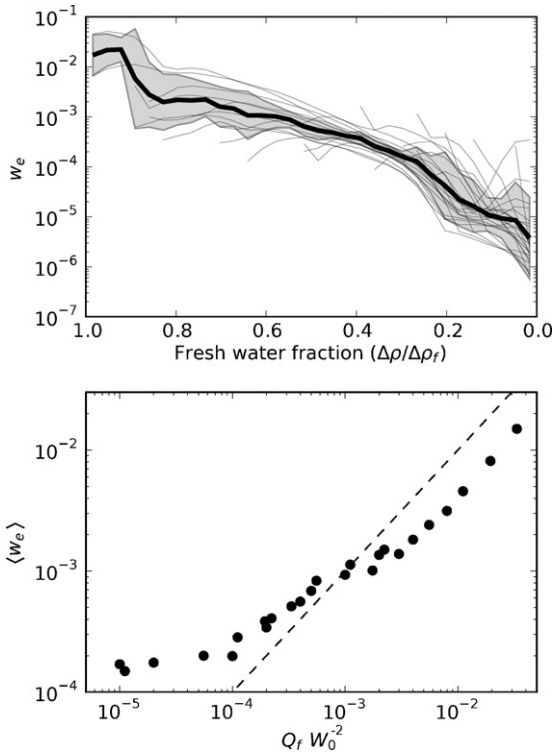

Fig. 3. The thin lines in the upper panel shows the entrainment velocity as a function of upper layer fresh water fraction, calculated using the isohaline method described in the text. The shading represents plus and minus one standard deviation from the mean, shown by the bold line. The bottom panel shows the *average* entrainment velocity in the first half of the plume as defined in density coordinates. This region is defined as the portion of the plume where the upper layer density is between the initial density at the estuary mouth and the value of density halfway between the initial and asymptotic density. The dashed line shows a 1:1 relationship.

where s_0 is the salinity of the background water (32 g kg^{-1} for the simulations presented here), and $\Delta\rho_f$ is the density difference between the fresh river water and the background water.

The upper panel of Fig. 3 shows the local entrainment velocity as a function of the upper layer density anomaly. This figure shows two important characteristics of entrainment in the three-dimensional model. First, the entrainment velocity decreases exponentially away from the source for all cases. Second, the entrainment at a particular density class does not depend on the initial density of the plume. (Note, the background salinity was not varied over these simulations, though Eq. (23) suggests that the value of the background salinity would also be an important factor in determining the entrainment velocity).

The lower panel of Fig. 3 shows $\langle w_e \rangle$ estimated from the three-dimensional model as a function of Q_f/W_0^2; W_0^2 was used as a scale for the plume area in Eq. (21). To calculate $\langle w_e \rangle$, the area between the initial density anomaly of the plume and the density anomaly corresponding to the mid-point between the initial and far-field asymptotic limit of the density anomaly was calculated. The entire plume was not used, since the average could be biased by the small entrainment rates and correspondingly large areas far from the source. Thus, $\langle w_e \rangle$ represents the average of the more energetic entrainment in the first half of the plume as defined in density space.

The lower panel of Fig. 3 demonstrates that the average entrainment velocity, $\langle w_e \rangle$, is proportional to the fresh water flux, Q_f, and inversely proportional to the square of initial plume width, W_0^2. This is notable because it might be expected that the entrainment rate is a function of the entire transport at the estuary mouth, Q_0, based on the derivations in the previous section. Rather, Eq. (21) suggests

Please cite this article in press as: Hetland, R.D., The effects of mixing and spreading on density in near-field river plumes. Dyn. Atmos. Oceans (2009), doi:10.1016/j.dynatmoce.2008.11.003

that it is rather the fresh water flux that is the primary factor determining mean entrainment rates although the upper panel of Fig. 3 suggests that the initial *local* entrainment rates are determined by the density anomaly of the plume.

4.4. Density changes in the near-field plume

Based on Eq. (15), and given that the non-dimensional system of equations has only one free parameter, δ/α_0, a plausible scaling for the density at the point where the plume returns to subcritical is

$$\frac{\Delta\rho_L}{\Delta\rho_0} = \Phi\left(\frac{\delta}{\alpha_0}\right) = \Phi\left(\frac{w_e W_0^2}{Q_0}\right), \tag{24}$$

where Φ is a function of unknown form. Here, the final values of W_L and Q_L in Eq. (18) have simply been replaced by W_0, the width of the estuary mouth, and Q_0, the mass flux at the estuary mouth.

The density anomaly of water leaving the near-field plume, the far-field density anomaly, is calculated in two ways. First, in the layer model, the far-field density anomaly is defined at the point where the plume returns to subcritical. The justification for this approach is that mixing will be greatly reduced once the plume has returned to subcritical – the Richardson number will be above one and turbulent mixing by shear instabilities will be suppressed. Also, the plume structure can be defined exactly by Eq. (18). However, in the three-dimensional model (as well as in observations), it is often difficult to define the *exact* point where the plume returns to subcritical. Also, while turbulent mixing is suppressed in the subcritical portion of the plume, it is never zero. For example, recent observations of turbulent dissipation in a dense gravity current show interfacial mixing even for Froude numbers of about 0.5 (Umlauf et al., 2007; Arneborg et al., 2007).

Thus, a second definition is used to define the far-field density anomaly of the plume that does not depend on the Froude number. This approach fits, in a least-squares sense, an exponential decay of the density anomaly, with the free parameters being the initial density anomaly, the asymptotic limit of the density anomaly, and the length-scale of decay. The functional form of this fit was determined by the fact that simulations and observations of plume structure show that the density anomaly often follows approximately this form (Fig. 2).

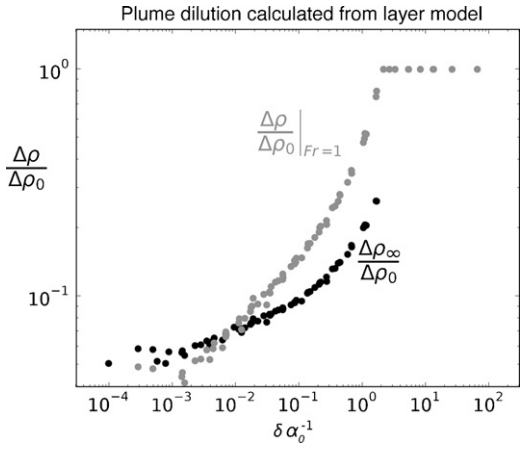

Fig. 4. The far-field density anomaly is shown for a wide range of input parameters (with $Fr_0 = 1$). Two definitions of the far-field density anomaly are shown: Black dots show the asymtotic density anomaly infinitely far from the source as determined by fitting the density anomaly to exponential decay. The gray dots show the value of the density anomaly at the point where the plume returns to subcritical. Values to the right of $\delta\alpha^{-1} = 2$ show that the density anomaly does not change in the plume; there is no supercritical outflow region.

Please cite this article in press as: Hetland, R.D., The effects of mixing and spreading on density in near-field river plumes. Dyn. Atmos. Oceans (2009), doi:10.1016/j.dynatmoce.2008.11.003

These two methods give the same functional dependence for the layer model; Fig. 4 shows the far-field density anomaly for a wide range of initial conditions listed in Table 1. Although this figure only shows simulations with $Fr_0 = 1$, this relationship also holds for different values of Fr_0 and different specifications of the entrainment. For $Fr \neq 1$, the functional relationship is between $Fr_0^{1/2}\Delta\rho/\Delta\rho_0$ and $Fr_0\delta/\alpha_0$ is identical to that plotted in Fig. 4.

Entrainment in the near-field plume may be parametrized by a number of different methods of increasing complexity: a constant entrainment ($w_e = \text{const.}$) does not consider local plume structure; a constant entrainment rate ($w_e/u = \text{const.}$) – the results presented here – considers changes in momentum, but not buoyancy, within the plume; finally, Richardson number dependent entrainment ($w_e = \mathcal{F}(Ri)$) could be used to consider changes in both momentum and buoyancy. All three entrainment parameterizations were tested within the layer model framework, with the Richardson number dependent entrainment based on Ellison and Turner (1959). For cases where the entrainment rate, δ, varied through the plume, a representative value for δ was used for scaling: δ_0 at $x = 0$ for the constant w_e case, or a minimum specified value for the Ellison and Turner parameterization (see Section 5 for more on this minimum specified value). For all of the definitions of the entrainment rate, the form functional dependence is slightly different but the tendencies are always the same – the far-field density anomaly is positively correlated with $\alpha\delta^{-1}$.

Although is possible to estimate an entrainment equivalent to w_e from the three-dimensional model results, it is not considered a robust parameter. Also, it is difficult to estimate w_e observationally without detailed, high-resolution turbulence or hydrographic measurements. Because of this, the far-field density anomaly is compared to two terms that do not depend on the entrainment velocity, but have similarities to Eq. (24). From the definition, $\delta/\alpha = w_e W_0^2 Q_0^{-1}$, it is likely that the density anomaly will be proportional to a horizontal length scale squared divided by a transport. The most reasonable choice for the horizontal length scale is W_0, however there are two reasonable choices for the transport scale: the total transport at $x = 0$, Q_0, and the fresh water flux, Q_f. The importance of the fresh water flux was demonstrated in Eq. (21).

Fig. 5 shows the far-field density anomaly compared to $W_0^2 Q_0^{-1}$ (that is, w_e is constant, or a function of $W_0^2 Q_0^{-1}$ in Eq. (24)) and $W_0^2 Q_f^{-1}$. The far-field density anomaly appears to be more closely related to $W_0^2 Q_f^{-1}$ indicating a functional independence with respect to entrainment velocity; the trend is similar for the relationship between the far-field density anomaly and $W_0^2 Q_f^{-1}$ but the correlation is not as tight. I believe Q_f is the right choice in scaling the transport because of the strong relationship between the entrainment velocity and the fresh water flux discussed in the previous section.

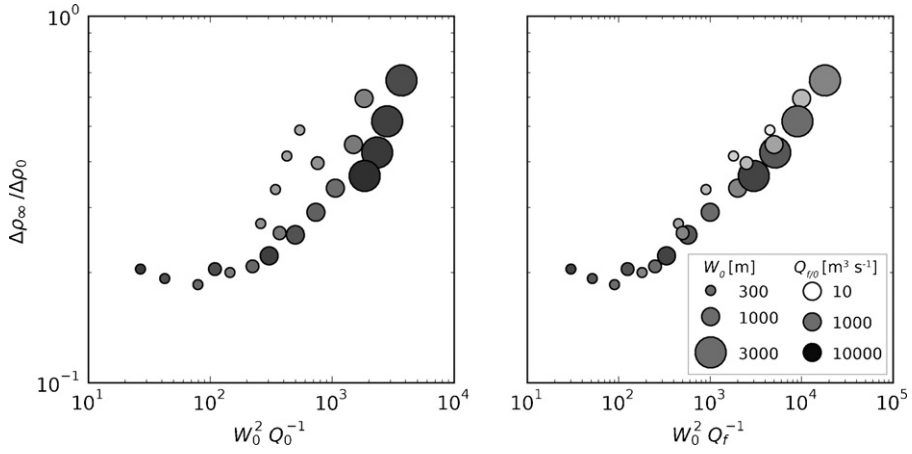

Fig. 5. The asymptotic density anomaly of the near-field plume is calculated by fitting the density structure to an exponential decay, and is plotted against W_0^2/Q_0 and W_0^2/Q_f.

Please cite this article in press as: Hetland, R.D., The effects of mixing and spreading on density in near-field river plumes. Dyn. Atmos. Oceans (2009), doi:10.1016/j.dynatmoce.2008.11.003

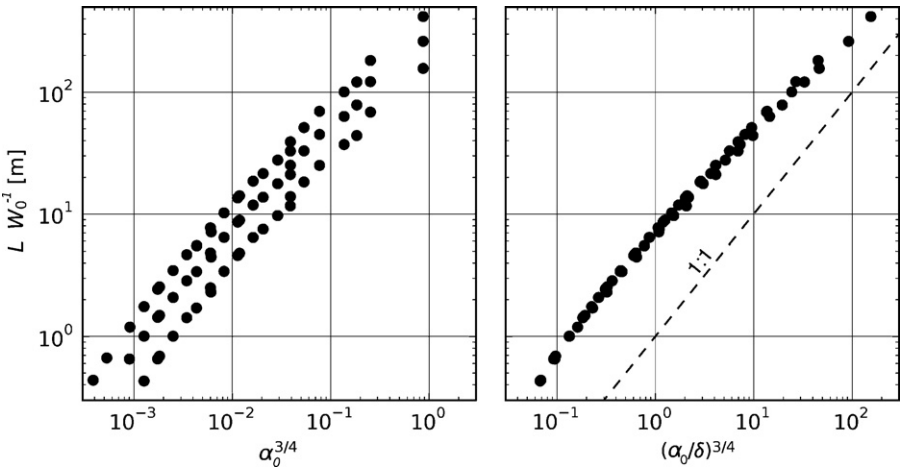

Fig. 6. The length scale, L/W_0, of density changes in the near-field plume layer model is calculated by fitting the density structure to an exponential decay. The normalized length scale is plotted against the initial aspect ratio of the plume, $(\alpha_0)^{3/4}$, and $\alpha/\delta^{3/4}$.

4.5. Length scale of the near-field plume

Length scales for engineering jets are based on the mass, momentum and buoyancy fluxes of the outflow (e.g., Fischer et al., 1979; Jones et al., 2007). In particular, the ratio of the momentum and buoyancy fluxes defines the distance from the source where buoyancy effects begin to become important relative to the initial inertia of the plume

$$L = \frac{M_0^{3/4}}{J_0^{1/2}} = \alpha_0^{3/4} W_0 \tag{25}$$

where $M_0 = u_0 Q_0$ is the momentum flux and $J_0 = g_0' Q_0$ is the buoyancy flux at the estuary mouth; this ratio is recast in terms of α_0 and W_0 for comparison to the density scale presented above. Note, Fr_0 is again assumed to be one in the right hand side of Eq. (25). For both the layer model and three-dimensional model, the length scale of the plume was calculated by using the exponential decay scale from the same calculation used to determine the asymptotic value of the density anomaly above, and plotted against Eq. (25).

Both the layer model (Fig. 6, left panel) and the three-dimensional model (Fig. 7, left panel) show a positive correlation between the normalized length scale, L/W_0 estimated from the momentum and buoyancy flux (Eq. (25)) and $\alpha^{3/4}$. The correlation between the predicted and estimated length scale for the layer model can be improved by multiplying Eq. (25) by $\delta^{-3/4}$ (Fig. 6, right panel). The rational for this is that δ/α_0 was shown to be a relevant parameter in determining the far-field density anomaly, so it is reasonable to assume it may also be relevant in determining the length scale. Indeed, this empirically determined relationship suggests that the form of turbulent closure, here in the form of the specified entrainment rate, affects the length scale of the plume. Note, in terms of the scales discussed in the previous section,

$$\frac{M_0^{3/4}}{J_0^{1/2}\delta^{3/4}} = \left(\frac{\delta}{\alpha_0}\right)^{-3/4} W_0. \tag{26}$$

Thus, both the net mixing within the near-field plume (Eq. (24)) and the length scale of the density anomaly depends inversely δ/α_0; i.e., inversely on the local mixing rate.

In the three-dimensional model results, the relevant parameter is $(Q_f W_0^{-2})^{1/2}$, the inverse of the scale shown to determine the far-field density anomaly. Given the relationship between δ/α_0 and the normalized length scale, L/W_0, in the layer model, and given the relationship between $W_0^2 Q_f^{-1}$ in

Please cite this article in press as: Hetland, R.D., The effects of mixing and spreading on density in near-field river plumes. Dyn. Atmos. Oceans (2009), doi:10.1016/j.dynatmoce.2008.11.003

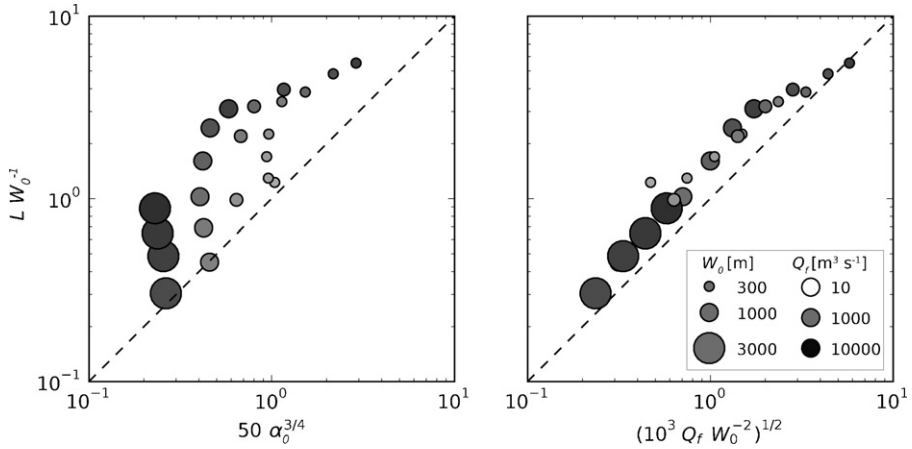

Fig. 7. The normalized length scale, L/W_0, of density changes in the near-field plume idealized three-dimensional model is calculated by fitting the density structure to an exponential decay. The length scale is plotted against $50\alpha_0^{3/4}$, and $10^3 Q_f W_0^{-2}$. The factors were chosen to give an approximate 1:1 relationship, shown by the dashed lines.

determining the far-field density anomaly, it seems reasonable that $Q_f W_0^{-2}$ would be the appropriate choice of variables that determine the length scale in the three-dimensional model. However, the power of the relationship changed from 3/4 to (approximately) 1/2. It is not yet clear why the power law dependence changes in the three-dimensional model, but it must be related to the differences in entrainment. The layer model results showed that entrainment was clearly a factor in determining the plume length. Here the relationship between entrainment through the parameter space is shown to be more complex than the simple constant entrainment rate specified in the layer model.

In both panels in Fig. 7, the abscissa has been multiplied by a factor to bring the displayed relationship to near 1:1. Note, a reasonable interpretation of the scale factor of 1000 in the right hand panel would be that it is the inverse of an entrainment velocity, $w_{e0} = 10^{-3}\ \mathrm{m\,s^{-1}}$. This interpretation is consistent with scale $\delta/\alpha_0 = w_e W_0^2 Q_0^2$ that has been shown to be relevant for the far-field density anomaly, it is dimensionally correct, and is similar in magnitude to the entrainment velocity estimated for a (nearly) pure fresh water plume at the estuary mouth (Fig. 3).

5. Discussion

Because of the simplified, idealized nature of the layer model, it does not reproduce many of the details of the near-field plume. To reproduce the structure of an individual plume, a more complex model such as presented by O'Donnell (1990) or Davis (1999) – or even better, a three-dimensional primitive equation model – should be used. Instead, the layer model presented here can be used to represent the scales of the plume over a broad range of mouth widths and discharge conditions, and gives some insight into the competing processes acting in the near-field plume. Thus, the layer model serves primarily as a scaling tool, a way to define the relevant parameter space and provide a context for analyzing the three-dimensional model results. The parameter space dependence of the layer model agrees well with that of the three-dimensional model, so the basic functional dependence of the net mixing and plume length scales described above appears to be robust. This means that the balance between mixing and spreading are shown to be the dominant factors in controlling plume structure: mixing acts to arrest the plume, spreading acts to intensify the plume.

There are two potentially important effects that were not examined in this paper, the effects of rotation and different entrainment parameterizations. Both the layer and three-dimensional models did not include the Coriolis effect. For typical near-field plume scales this effect is often probably small, but present. Hetland and MacDonald (2008) show that rotation turns the streamlines in the near-field to the right slightly, but rotation is not a primary factor in the near-field plume dynamics.

Please cite this article in press as: Hetland, R.D., The effects of mixing and spreading on density in near-field river plumes. Dyn. Atmos. Oceans (2009), doi:10.1016/j.dynatmoce.2008.11.003

However, although the near-field plume is not in a geostrophic balance, there may be some important secondary effects. For example, as the plume slows and rotational effects become more important, spreading may be arrested as the plume transitions from a spreading jet to a geostrophic current. This in turn could affect the net mixing that occurs over the near-field region. Recirculation of the larger, far-field plume (Fong, 1998; Yankovsky and Chapman, 1997; Horner-Devine et al., 2006) may also influence the near-field plume structure.

This paper did not explore how different parameterizations of mixing and entrainment affect the near-field plume structure in detail. A constant entrainment rate was used in the analytical discussion of the layer model because it is simple and analytically tractable. A Richardson number dependent entrainment could also be used with similar numerical parameter space results, but without the analytical insight. It should also be noted that the layer model solutions show that the Froude number is always $\mathcal{O}(1)$, and entrainment parameterizations do not well resolve differences in entrainment over such a small range of the Richardson number (e.g., Turner, 1973; Fernando, 1991; Cenedese and Adduce, 2008). Thus, it is not clear *a priori* that a Richardson number dependent entrainment would supply better results despite being physically more realistic. For example, in the layer model, any parameterization of entrainment in the near-field plume must include some entrainment when the flow is critical or near critical. For example, in the entrainment parameterization described by Ellison and Turner (1959), positive entrainment is only defined for values of the internal Froude number above 1.12 (or, a bulk Richardson number below 0.8). When this parameterization is used for the near-field plume, the Froude number remains at the critical value, as there is no way to reduce the Froude number further once the mixing has been suppressed. Thus, a minimum 'background' mixing needs to be specified. Curiously, the solutions using a constant entrainment rate mimic the three-dimensional numerical simulations closer than classic Froude number dependent entrainment parameterizations like Ellison and Turner (1959).

Different entrainment parameterizations, such as w_e = constant or Ellison and Turner (1959), were also examined in the layer model, though the results are not presented here. Different entrainment parameterizations obviously influence the solution. But the important point is that all entrainment parameterizations tested produce the same functional dependence; the details of the functional form do change, as expected, but the functional dependence and the functional tendencies do not. The net plume dilution is still a function of $w_e W_0^2 Q_0^{-1} = \delta\alpha_0^{-1}$, regardless of the entrainment parameterization used (provided a suitable scale for w_e is used), and lower local mixing always results in more net mixing within the plume. Thus, the primary results are independent of the form of entrainment parameterization. This is good, because entrainment parameterization is by far the least understood process in the layer model.

The three-dimensional model is also sensitive to the form of the entrainment parameterization, here the second-moment turbulence closure scheme (see, e.g., Umlauf and Burchard, 2005). As there is no stress at the free surface, and the flow is far from the bottom boundary, it is primarily the critical gradient Richardson number that determines the magnitude of shear mixing. The results presented use the Canuto A stability functions (Canuto et al., 2001), which reproduced observed turbulence dissipation values in a realistic numerical simulation reasonably well MacDonald et al. (2007). Although qualitatively similar, the details of mixing in the near-field plume can be quite different depending on the form of the closure used. Although the Canuto A formulation appears to be a reasonable choice, it is not yet clear if other choices would be better.

Only purely fresh water was introduced into the three-dimensional model, as this is how buoyancy fluxes are specified in realistic numerical simulations of coastal circulation. Numerical results presented in Fig. 5 show that the structure of entrainment in the three-dimensional model is related to the fresh water flux into the system, as opposed to the transport at the estuary mouth – a larger, denser transport due to entrainment within the estuary. This is because fresh water flux, relative to a particular isopycnal, can only cross that isopycnal via mixing, as described in Eqs. (21) and (22). Although the transport at the estuary mouth was greater than the fresh water flux, due to entrainment within the estuary, the entrainment in the plume beyond the estuary was correlated with the fresh water flux. That means that entrainment within the estuary had an impact on the subsequent plume structure. It is not yet fully clear why this relationship holds, but it seems that the estuary and near-field plume should be considered together, as a system.

Please cite this article in press as: Hetland, R.D., The effects of mixing and spreading on density in near-field river plumes. Dyn. Atmos. Oceans (2009), doi:10.1016/j.dynatmoce.2008.11.003

There has been much work examining engineering-scale jets and plumes, and this provides an excellent framework for analyzing geophysical scale plumes. For example, the length scale of the geophysical-scale near-field plume was shown to be related to a ratio of the momentum and buoyancy fluxes at the source, similar to an engineering-scale jet. However, there are some important differences between these two types of plumes. Perhaps the most fundamental difference between geophysical and engineering-scale jets and plumes is the aspect ratio of the plume cross-section. Often, for engineering-scale plumes (Fischer et al., 1979; Jirka, 1982; Davis, 1999; Jones et al., 2007), the aspect ratio of the source is generally assumed to be close to $\mathcal{O}(1)$. In this case, entrainment can occur both vertically and laterally in the case of a surface-trapped buoyant plume. For the geophysical case, the aspect ratio is much smaller. Because of this, entrainment occurs overwhelmingly through vertical mixing; lateral mixing may be neglected.

6. Conclusions

The primary result of this paper is that the net mixing within the near-field plume, determined by $\Delta\rho|_{Fr=1}$ or $\Delta\rho_\infty$ in Figs. 4 and 5, depends on $W_0^2 w_e Q_0^{-1} = \delta\alpha_0^{-1}$. The term $W_0^2 w_e Q_0^{-1}$ may be described as the ratio of water entrained over an area W_0^2 normalized by the volume transport out of the estuary. The term $\delta\alpha_0^{-1}$ may also be related to the integrated entrainment laterally across the plume at the source. Laterally integrated entrainment of course increases as the local entrainment rate, δ, increases, but decreases as the aspect ratio of the plume source, α_0, increases. This is because a shallow, wide plume will entrain more than a deep, narrow plume given the same local entrainment rate; the surface over which water may be entrained is simply larger in the shallow plume.

The parameter dependence of the net mixing throughout the entire near-field plume is at first unintuitive; the *net* mixing is inversely proportional to the *local* entrainment rate. Increasing δ, or decreasing α, will increase the density anomaly of water leaving the near-field plume, meaning that the total entrainment across the entire plume is less. This is because of the competition between mixing and spreading. If local mixing is weak, the spreading tendency of the plume will dominate and increase the Froude number. This means that even more net mixing will eventually be required to bring the plume back down to subcritical values. Conversely, if local mixing is high, the Froude number will quickly return to subcritical. Greater local mixing means that the development of the plume is quickly shut down resulting in a smaller plume; weaker mixing means that spreading and the associated acceleration of the upper layer has more of a chance to take hold resulting in a larger plume. On the other hand, the parameter dependence of the length scale of the density anomalies is more straightforward; as local mixing increases, the length scale of the plume decreases as expected.

Numerical results using a layer model of the near-field plume and three-dimensional ocean model confirm this scaling over a very wide range of parameters. The numerical results are also independent of the exact definition of the far-field density anomaly, and are valid for a number of different layer model and three-dimensional model configurations even beyond those shown in this paper.

References

Armi, L., Farmer, D.M., 1986. Maximal two-layer exchange through a contraction with barotropic net flow. J. Fluid Mech. 164, 27–51.
Arneborg, L., Fiekas, V., Umlauf, L., Burchard, H., 2007. Gravity current dynamics and entrainment—a process study based on observations in the Arkona Basin. J. Phys. Oceanogr. 37, 2094–2113.
Baines, P.G., 1995. Topographic Effects in Stratified Flows. Cambridge University Press.
Burchard, H., Bolding, K., 2001. Comparative analysis of four second-moment turbulence closure models for the oceanic mixed layer. J. Phys. Oceanogr. 31, 1943–1968.
Burchard, H., Rennau, H., 2008. Comparative quantification of physically and numerically induced mixing in ocean models. Ocean Model. 20 (3), 293–311.
Canuto, V.M., Howard, A., Cheng, Y., Dubovikov, M.S., 2001. One-point closure model—momentum and heat vertical diffusivities. J. Phys. Oceanogr. 31, 1413–1426.
Cenedese, C., Adduce, C., 2008. Mixing in a density-driven current flowing down a slope in a rotating fluid. J. Fluid Mech. 604, 369–388.
Cenedese, C., Whitehead, J.A., Ascarelli, T.A., Ohiwa, M., 2004. A dense current flowing down a sloping bottom in a rotataing fluid. J. Phys. Oceanogr..
Chatwin, P.C., 1976. Some remarks on the maintenance of the salinity distribution in estuaries. Estuar. Coast. Mar. Sci. 4, 555–566.

Please cite this article in press as: Hetland, R.D., The effects of mixing and spreading on density in near-field river plumes. Dyn. Atmos. Oceans (2009), doi:10.1016/j.dynatmoce.2008.11.003

Davis, L.R., 1999. Fundamentals of Environmental Discharge Modeling. CRC Press.
Ellison, T.H., Turner, J.S., 1959. Turbulent entrainment in stratified flows. J. Fluid Mech. 6, 423–448.
Fernando, H.J.S., 1991. Turbulent mixing in stratified fluids. Annu. Rev. Fluid Mech. 23, 455–493.
Fischer, H.B.E., List, J., Koh, R.C., Imberger, J., Brooks, N.H., 1979. Mixing in Inland and Coastal Waters. Academic Press, San Diego.
Fong, D.A., 1998. Dynamics of freshwater plumes: observations and numerical modeling of the wind-forced response and alongshore freshwater transport. Ph.D. Thesis. Joint Program in Oceanography, MIT/WHOI.
Fong, D.A., Geyer, W.R., 2001. Response of a river plume during an upwelling favorable wind event. J. Geophys. Res. 106 (C1), 1067–1084.
Fong, D.A., Geyer, W.R., 2002. The alongshore transport of freshwater in a surface-trapped river plume. J. Phys. Oceanogr. 32, 957–972.
Garvine, R.W., 1982. A steady state model for buoyant surface plume hydrodynamics in coastal waters. Tellus 34, 293–306.
Garvine, R.W., 1984. Radial spreading of buoyant, surface plumes in coastal waters. J. Geophys. Res. 89 (C2), 1989–1996.
Garvine, R.W., 1987. Estuary plumes and fronts in shelf waters: a layer model. J. Phys. Oceanogr. 17, 1877–1896.
Garvine, R.W., 1999. Penetration of buoyant coastal discharge onto the continental shelf: a numerical study. J. Phys. Oceanogr. 29, 1892–1909.
Hansen, D.V., Rattray, M., 1965. Gravitational circulation in straits and estuaries. J. Mar. Res. 23, 104–122.
Hetland, R.D., 2005. Relating river plume structure to vertical mixing. J. Phys. Oceanogr. 35 (9), 1667–1688.
Hetland, R.D., Geyer, W.R., 2004. An idealized study of long, partially mixed estuaries. J. Phys. Oceanogr. 34 (12), 2677–2691.
Hetland, R.D., MacDonald, D.G., 2008. Spreading in the near-field Merrimack river plume. Ocean Model. 21, 12–21.
Horner-Devine, A.R., Fong, D.A., Monismith, S.G., Maxworthy, T., 2006. Laboratory experiments simulating a coastal river discharge. J. Fluid Mech. 555, 203–232.
Jirka, G.H., 1982. Turbulent buoyant jets in shallow fluid layers. In: Rodi, W. (Ed.), Turbulent Buoyant Jets and Plumes. Pergamon Press, p. 184.
Jones, G.R., Nash, J.D., Doneker, R.L., Jirka, G.H., 2007. Buoyant surface discharges into water bodies. I: flow classification and prediction methodology. J. Hydraul. Eng. 133 (9), 1010–1020.
Lentz, S.J., Helfrich, K.R., 2002. Buoyant gravity currents along a sloping botton in a rotating fluid. J. Fluid Mech. 464, 251–278.
Luketina, D., Imberger, J., 1987. Characteristics of a suface buoyant jet. J. Geophys. Res. 92 (C5), 5435–5447.
MacCready, P., 2007. Estuarine adjustment. J. Phys. Oceanogr. 37, 2133–2145.
MacCready, P., Hetland, R.D., Geyer, W.R., 2002. Long-term isohaline salt balance in an estuary. Cont. Shelf Res. 22, 1591–1601.
MacDonald, D.G., Geyer, W.R., 2004. Turbulent energy production and entrainment at a highly stratified estuarine front. J. Geophys. Res. 109, C05004.
MacDonald, D.G., Geyer, W.R., 2005. Hydraulic control of a highly stratified estuarine front. J. Phys. Oceanogr. 35 (3), 374–387.
MacDonald, D.G., Goodman, L., Hetland, R.D., 2007. Turbulent dissipation in a near-field river plume: a comparison of control volume and microstructure observations with a numerical model. J. Geophys. Res. 112, C07026.
McCreary, J.P., Zhang, S., Shetye Jr., S.R., 1997. Coastal circulations driven by river outflow in a variable-denisty 1 1/2-layer model. J. Geophys. Res. 102 (C7), 15,535–15554,15554.
O'Donnell, J., 1990. The formation and fate of a river plume: a numerical model. J. Phys. Oceanogr. 20 (4), 551–569.
Shchepetkin, A.F., McWilliams, J.C., 2005. The regional oceanic modeling system (ROMS): a split-explicit, free-surface, topographically-following-coordinate oceanic model. Ocean Model. 9, 347–404.
Stommel, H., Farmer, H.G., 1953. Control of salinity in an estuary by a transition. J. Mar. Res. 12 (1), 12–20.
Turner, J.S., 1973. Buoyancy Effects in Fluids. Cambridge University Press.
Umlauf, L., Burchard, H., 2005. Second-order turbulence closure models for geophysical boundary layers. A review of recent work. Cont. Shelf Res. 25, 795–827.
Umlauf, L., Arneborg, L., Burchard, H., Fiekas, V., Lass, H.U., Mohrholz, V., Prandke, H., 2007. Transverse structure of turbulence in a rotating gravity current. Geophys. Res. Lett. 34.
Warner, J., Geyer, W.R., Lerczak, J., 2005. Numerical modeling of an estuary: a comprehensive skill assessment. J. Geophys. Res. 110 (C05001).
Wright, L.D., Coleman, J.M., 1971. Effluent expansion and interfacial mixing in the presence of a salt wedge, Mississippi River Delta. J. Geophys. Res. 76 (36), 8649–8661.
Yankovsky, A.E., Chapman, D.C., 1997. A simple theory for the fate of buoyant coastal discharges. J. Phys. Oceanogr. 27, 1386–1401.

Please cite this article in press as: Hetland, R.D., The effects of mixing and spreading on density in near-field river plumes. Dyn. Atmos. Oceans (2009), doi:10.1016/j.dynatmoce.2008.11.003